Vibrational properties of 2H-PbI2 semiconductors studied via Density Functional Theory calculations

Laurent Pedesseau, Jacky Even, Claudine Katan, Faical Raouafi, Y. Wei, Emmanuelle Deleporte, Jean-Marc Jancu

Vibrational properties of 2H-PbI_2 semiconductors studied via Density Functional Theory calculations

L. Pedesseau [a),*], J. Even [a)], C. Katan [a,b)], F. Raouafi [c)]Y. Wei [d)], E. Deleporte [d)] and J.-M. Jancu [a)]

[a)] Université Européenne de Bretagne, INSA, FOTON, UMR CNRS 6082, 20 Avenue des Buttes de Coësmes, F-35708 Rennes, France

[b)] CNRS, Institut des Sciences Chimiques de Rennes, UMR 6226, 35042 Rennes, France

[c)] Laboratoire de Physico-chimie des matériaux polymères, Institut Préparatoire aux Etudes Scientifiques et Techniques, BP51, 2070 La Marsa, Tunisia

[d)] Laboratoire de Photonique Quantique et Moléculaire, Ecole Normale Supérieure de Cachan, 61 Avenue du Président Wilson, 94 235 Cachan Cedex, France

Abstract.

Density functional theory is used to study the vibrational properties of 2H-PbI_2 semiconductor. The Born charge tensors are determined. Calculated phonon frequencies at the Brillouin zone center are compared to Raman scattering and IR absorption measurements. The computed Raman spectra show a good agreement with available experimental data. The simulated phonon dispersion curves are compared with triple-axis neutron scattering measurements.

Keywords:

DFT, vibrational properties, semiconductor

* Corresponding author. E-mail address: laurent.pedesseau@insa.rennes.fr

1. Introduction

Today, inorganic-organic hybrid quantum structures represent innovative routes in solid-state chemistry and optoelectronic devices [1]. Applications include all-optical nonlinear functionalities built upon the exciton-photon coupling in microcavity architectures [2, 3], high power light emitting diodes [4], and nanoelectronics [1].

Although there is a surge of interest in the physical properties of low-dimensional lead iodide compounds, there is little information regarding the inorganic counterpart PbI_2. It is known that PbI_2 is a layered semiconductor involving an atomic layer of Pb sandwiched between two layers of I atoms. The atomic structure can be stacked in variety of forms [5] due to the weak forces between sheets. Actually, the most common structure is the 2H trigonal polytype [6]. Indeed, similar dispersion curves can be considered for higher polytypes, but folding of phonons branches is associated to larger cells along the c axis. The choice of 2H-PbI_2 was then also motivated by the reduction of the computational resources needed to perform the phonon simulation. Such an effect of polytypes on the vibrational properties at q=0 has also been studied for the SiC material. [7-8] Concerning the experimental side, bulk 2H-PbI_2 has encompassed various studies ranging from Raman spectroscopy [9-12], and X-ray photoemission spectra [6, 13-17]. Conversely, theoretical approaches so far have been concerned with only few empirical works [18, 19] and a detailed insight from the first-principles approach is still lacking.

In this paper, we present Density Functional Theory (DFT) and Density Functional Perturbation Theory calculations (DFPT) [20-22] of dynamical properties of 2H-PbI_2. The paper is organized into 4 sections. Section 2 gives details on the numerical computation. Section 3 presents the study of the vibrational and dielectric properties. Section 4 is a conclusion.

2. Computational details

Total energy DFT calculations are carried out by means of the state of the art ABINIT code [22] within the local density approximation (LDA) [23]. A plane-wave basis set with an energy cut-off of 950 eV is used to expand the electronic wave-functions. The reciprocal space integration is performed over 12x12x8 Monkhorst-Pack grid [24, 25]. The energy is computed from the linear response method [22] and convergence is accurately reached with tolerance on the residual potential which stems from differences between the input and output potentials. The crystal structure is relaxed until the forces acting on each atom are smaller than 5.10^{-5} eV/Å. The pseudopotentials are constructed from the Fritz Haber Institute (FHI) [26] format using the OPIUM code (G. G. P. Licence, version 3.6 (10/2012)) [27] for Pb [$6s^2 6p^2 5d^{10}$] atom and for I [$5s^2 5p^5$] atoms. The vibrational properties are studied from the density functional perturbation theory (DFPT) based on the linear response. The so-called 2n+1 theorem [28] within DFPT provides a direct access to the second-order and third-order response functions and has been extensively used for semiconductors in the calculation of total-energy related properties [29-31].

3. Dynamical properties

3.1 Symmetry analysis at the Brillouin zone center

The analysis of the vibrational properties takes into account the atomic positions in the unit cell. The total mechanical representation M is derived from the Wyckoff positions **1a**, and **2d** of the Pb, and I atoms respectively. The 9 vibrational modes of 2H-PbI_2 decompose into the irreducible representations of D_{3d} point group:

$$M = A_{1g} + 2A_{2u} + 2E_u + E_g$$

where E_u and E_g representations are twice degenerated. The three acoustic modes correspond to the A_{2u}+E_u representation. The 6 optical modes (A_{1g}+A_{2u}+E_g+E_u) decomposed into 3 infrared active polar modes (A_{2u}+E_u) and 3 Raman active unipolar modes (A_{1g}+E_g). Figure 1

illustrates the atomic motions for the various Infrared and Raman modes. Due to its special position, the Pb atom is motionless for unpolar modes.

3.2 Polar modes and infrared spectroscopy results

DFPT gives the opportunity to compute the Longitudinal Optical - Transverse Optical (LO-TO) splitting associated to polar modes. A previous experimental study by infrared spectroscopy [9], has indeed shown that the LO-TO splitting is especially large in the 2H-PbI_2 crystal with peaks located in the far-infrared spectral range at 52 (E_u(TO)), 95 (A_{2u}(TO)), 109 (E_u(LO)) and 110 cm^{-1} (A_{2u}(LO)). The DFPT computations yields frequencies equal to 64.4 cm^{-1} (E_u(TO)), 111.7 cm^{-1} (A_{2u}(TO)), 115.5 cm^{-1} (E_u(LO)), and 125.8 cm^{-1} (A_{2u}(LO)). Computed frequencies are shifted by about 10-15 cm^{-1} with respect to experimental ones. This may be partly attributed to the effect of temperature. DFPT results are indeed computed at T=0K, whereas experimental results are either obtained at T=77K or room temperature. The experimental large values of the E_u and A_{2u} LO-TO splittings are nevertheless very well explained by the theoretical modelling.

3.3 Dielectric tensors

The DFPT theoretical approach gives also access to the variation of the dielectric tensors related to lattice polarisability: $\varepsilon_{ij}^{s} = \varepsilon_{ij}^{ion} + \varepsilon_{ij}^{\infty}$, where the static ε_{ij}^{s} and high-frequency $\varepsilon_{ij}^{\infty}$ dielectric tensors are defined. The ε_{ij}^{ion} ionic contribution is associated to the polar modes studied in section 3.2. The observed very large anisotropy of this contribution is very well reproduced by the simulations as shown in Table I.

3.4 Unpolar modes and Raman spectroscopy

DFPT modelling of the 2H-PbI_2 crystal yields two unipolar E_g and A_{1g} modes (figure 1) with frequencies equal to 81 and 97 cm^{-1} respectively at T=0K. This is in good agreement with previous measurements which give peaks located at about 79 and 98 cm^{-1} at T=4.2K [9], and 74 and 95 cm^{-1} at room temperature 293K [12].

Raman spectra can be computed the linear response method, for light polarizations parallel (H) or orthogonal (V) to the incident one. HH component of the Raman tensors is then computed for a polycrystalline sample, by averaging over all the possible orientations. The Raman susceptibility α^{v} tensors are calculated using standard definitions [33, 34] for a given vibrational eigenmode v:

$$\alpha_{ij}^{v} = \sqrt{\Omega}\sum_{n}\sum_{l}\frac{\partial\chi_{ij}}{\partial r_{l}}\bigg|_{n}\frac{\xi_{nl}^{v}}{\sqrt{m_{n}}}, \begin{cases} n \equiv Pb, I \\ i, j, l \equiv x, y, z \end{cases}$$

where Ω is the volume of the primitive cell, χ_{ij} is the dielectric susceptibility tensor, r_l is the displacement of n along the Cartesian axes, m_n is the mass of n, and ξ_{nl}^{v} the normalized eigenmode of the atom n in the vibrational mode v. The calculation of the derivatives of the dielectric polarization tensor is the more demanding computational part. Figure 2 shows that the computed Raman spectrum is in good agreement with experimental measurements [9].

3.5 Phonon dispersion and neutron scattering measurements

Figure 3 shows the experimental (triangles, neutron scattering at room temperature [35]) and computed (straight lines, T=0K) phonon dispersion curves of 2H-PbI_2. The three acoustic branches are located in the [0-50cm^{-1}] low-frequency range. A good agreement is again obtained between experimental and theoretical results, except for a slight overestimation of sound velocities which may be attributed to the temperature effect on the elastic constants. Neutron scattering experiments [35] have only given results for the lowest energy optical phonon branch. It corresponds to the E_u mode at the Brillouin zone center, in good agreement with the study of polar modes (see section 3.2).

4. Conclusion

A theoretical analysis of the vibrational properties of 2H-PbI_2 crystal lattice has been presented with comparisons to available experimental data. A symmetry analysis and a

computation of the dynamical matrix at the Brillouin zone center are performed. The polar modes, LO-TO splittings and dielectric tensors are studied. The computed Raman scattering spectra are in good agreement with experimental results. Phonon dispersion curves are compared with triple axis neutron scattering measurements.

Acknowledgments

The DFT simulations have been performed on HPC resources of CINES and IDRIS under the allocation 2012-[x2012096724] made by GENCI (Grand Equipement National de Calcul Intensif). This work was supported in part by the ANR project PEROCAI (10-04) and the PHC UTIQUE 2011

[1] C. R. Kagan, D. B. Mitzi, and C. D. Dimitrakopoulos. Science. 286 (1999) 945

[2] G. Lanty, A. Brehier, M. Parashkov, J. S. Lauret, and E. Deleporte. New Journal of Physics. 10 (2008) 065007

[3] C. Weisbuch, M. Nishioka, A. Ishikawa, and Y. Arakawa, Phys. Rev. Lett. 69 (1992) 3314

[4] R. B. Fletcher, D. G. Lidzey, D. D. C. Bradley, M. Bernius, and S. Walker, Appl. Phys. Lett. 77 (2000) 1262

[5] A. R. Verma and P. Krishna, Polymorphism and Polytypism in Crystals (New York: Wiley, 1966)

[6] R. S. Mitchell, Zeitschrift für Kristallographie, 117 (1962) 309

[7] L. Patrick, Phys. Rev. 167 (1968) 809

[8] D. W. Feldman, J. H. Parker, Jr., W. J. Choyke, and L. Patrick, Phys. Rev. 170 (1968) 698

[9] A. Grisel and P. Schmid, physica status solidi (b) 73 (1976) 587

[10] A. Dugan and H. Henisch, J. of Physics and Chemistry of Solids 28 (1967) 971

[11] W. M. Sears, M. L. Klein, and J. A. Morrison, Phys. Rev. B 19 (1979) 2305

[12] B. Winkler, M. Dove, E, Salje, M. Leslie, and B. Palosz, J. of Physics: Condensed Matter 3 (1991) 539

[13] C. Gähwiller and G. Harbeke, Phys. Rev. 185 (1969) 1141

[14] C. Ghita, L. Ghita, I. Baltog, and M. Constantinescu, Physica Status Solidi (b) 102 (1980) 111

[15] Y. Nagamune, S. Takeyama, and N. Miura, Phys. Rev. B 40 (1989) 8099

[16] L. C. Thanh, C. Depeursinge, F. Levy, and E. Mooser, J. Phys. Chem. Solids 36 (1975) 699

[17] M. Scrocco, J. of Electron Spectroscopy and Related Phenomena, 48 (1989) 363

[18] I. C. Schlüter and M. Schlüter, Phys. Rev. B 9 (1974) 1652

[19] Y.-C. Chang and R. B. James, Phys. Rev. B 55 (1997) 8219

[20] W. Kohn and L. J. Sham, Phys. Rev. 140 (1965) A1133

[21] R. Martin, Electronic Structure: Basic Theory and Practical Methods (Cambridge University Press, 2004)

[22] X. Gonze, J.-M. Beuken, R. Caracas, F. Detraux, M. Fuchs, G.-M. Rignanese, L. Sindic, M. Verstraete, G. Zerah, F. Jollet, M. Torrent, A. Roy, M. Mikami, P. Ghosez, J.-Y. Raty, and D. Allan, Computational Materials Science 25 (2002) 478

[23] J. P. Perdew and Y. Wang, Phys. Rev. B 45 (1992) 13244

[24] H. J. Monkhorst and J. D. Pack, Phys. Rev. B 13 (1976) 5188

[25] J. D. Pack and H. J. Monkhorst, Phys. Rev. B 16 (1977) 1748

[26] M. Fuchs and M. Scheffler, Computer Physics Communications 119 (1999) 67

[27] I. Grinberg, N. Ramer, A. Rappe, Phys. Rev. B 62 (2000) 2311

[28] X. Gonze and J.-P Vigneron, Phys. Rev. B 39 (1989) 13120

[29] P. Giannozzi, S. de Gironcoli, P. Pavone, and S. Baroni, Phys. Rev. B 43 (1991) 7231

[30] X. Gonze and C. Lee, Phys. Rev. B 55 (1997) 10355

[31] S. Baroni, S. de Gironcoli, A. Dal Corso, and P. Giannozzi, Rev. Mod. Phys. 73 (2001) 515

[32] G. Lucovsky, R. White, W. Liang, R. Zallen, and P. Schmid, Solid. State. Communications 18 (1976) 811

[33] M. Cardonna and G. Güntherodt, Light scattering in solids II: basic concepts and instrumentations (Springer-Verlag Berlin and Heidelberg GmbH & Co. K,1982)

[34] R. Loudon, Advances in Physics, 13 (1964) 423

[35] B. Dorner, R. E. Ghosh, and G. Harbeke, Physica Status Solidi (b), 73 (1976) 655

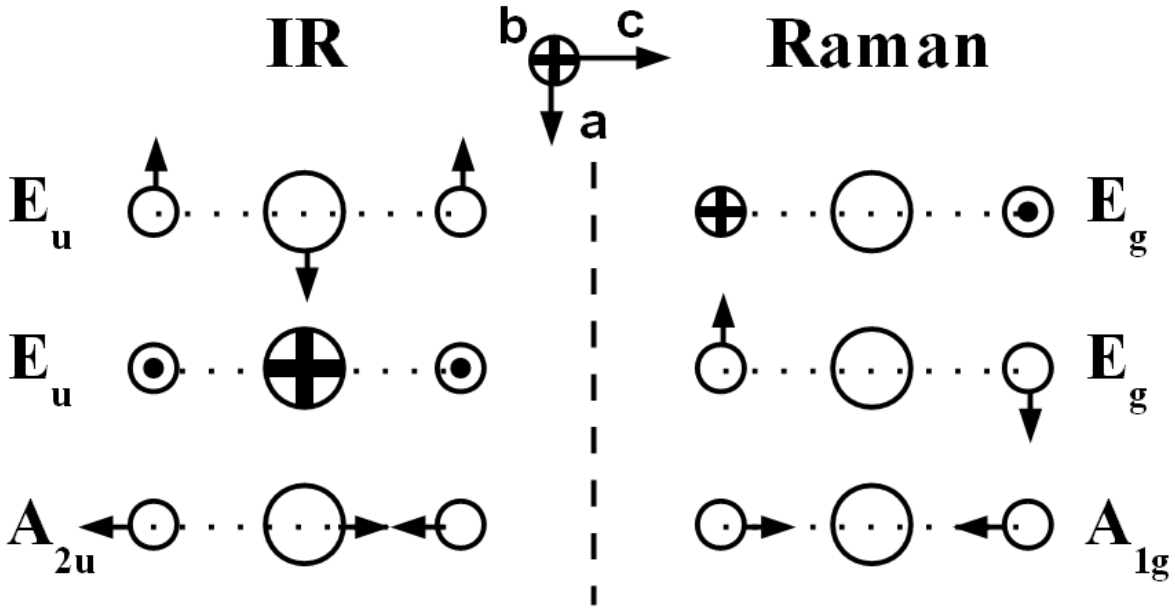

Figure 1: Schematic representation of the atomic motions for the various optical modes

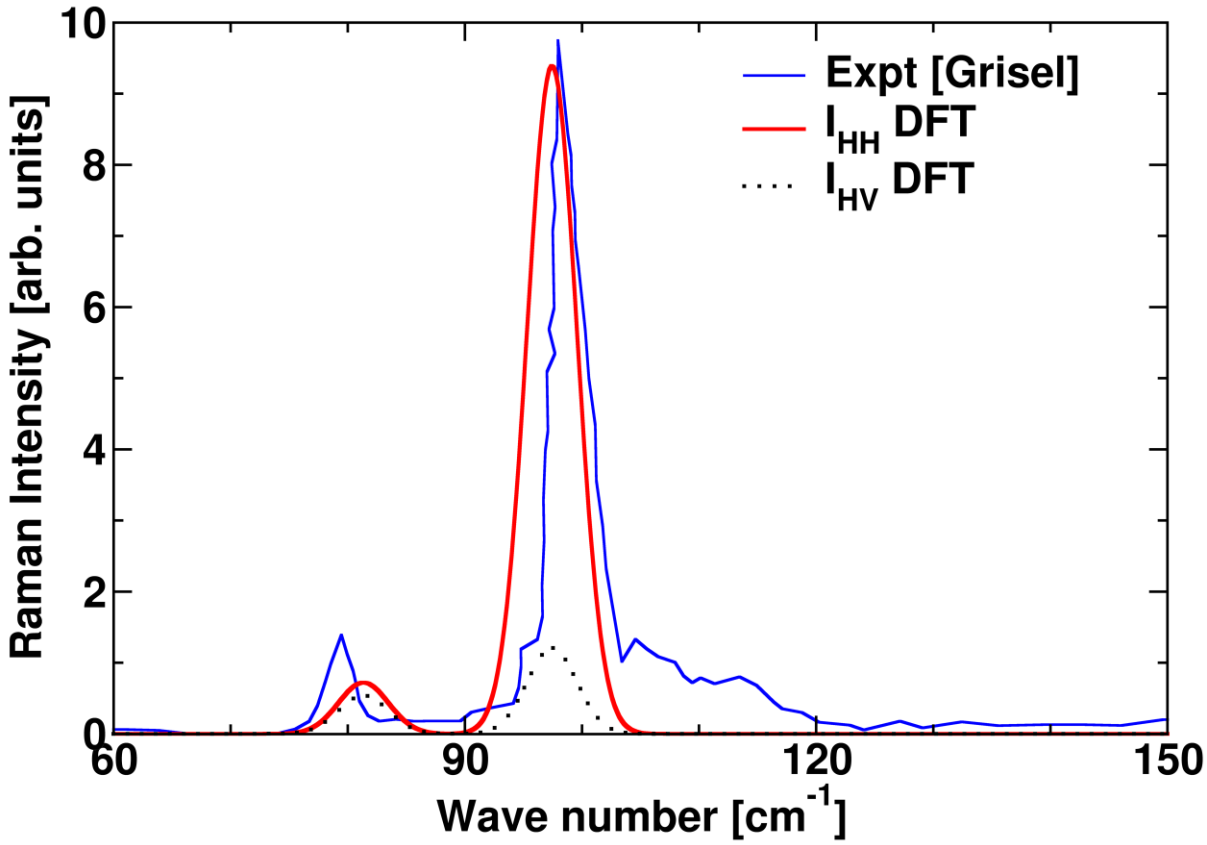

Figure 2: Computed Raman spectrum (red line) compared to experimental measurements ([9], blue line)

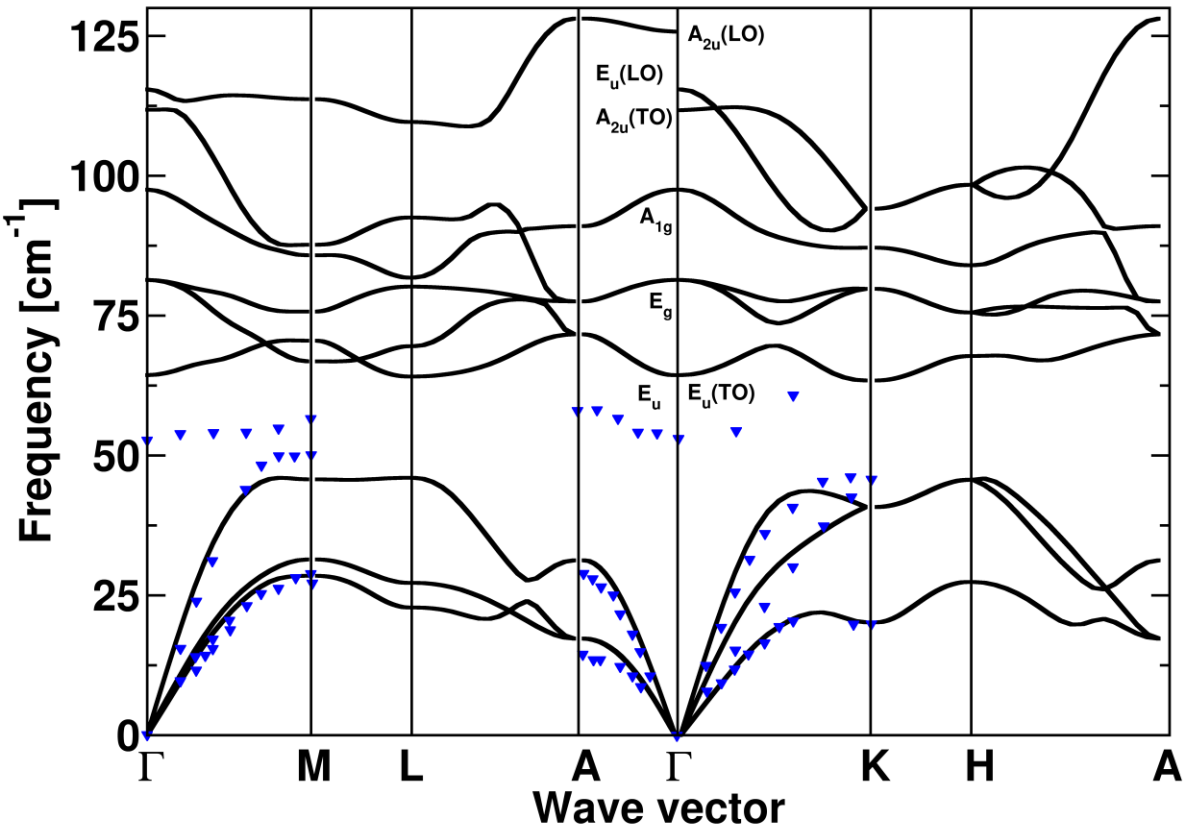

Figure 3: Experimental (triangles, neutron scattering at room temperature [35]) and computed (straight lines, T=0K) phonon dispersion curves of 2H-PbI_2

	$\|\|$ modes	$\perp$ modes
$\varepsilon_{\bullet}^{ion}$	15.77	1.19
$\varepsilon_{\bullet}^{ion}$ Expt [9]	20.5	0
$\varepsilon_{\bullet}^{ion}$ Expt [33]	20.3	1.9
$\varepsilon_{\bullet}^{\infty}$	7.85	6.32
$\varepsilon_{\bullet}^{\infty}$ Expt [9,10]	6.25/6.21	6.25/6.21
$\varepsilon_{\bullet}^{\infty}$ Expt [32]	6.1	6.1
$\varepsilon_{\bullet}^{S}$	23.62	7.51
$\varepsilon_{\bullet}^{S}$ Expt [9]	26.75	6.25
$\varepsilon_{\bullet}^{S}$ Expt [32]	26.4	8.0

Table I

DFT global contributions $\varepsilon_{\bullet}^{ion}$, the electronic part $\varepsilon_{\bullet}^{\infty}$, and the static dielectric constants $\varepsilon_{\bullet}^{S}$ compared to measurements [9,10, 32] (with $\bullet \equiv \|, \perp$).